Acta Crystallographica Section F
Structural Biology and Crystallization Communications
ISSN 1744-3091

Purification, crystallization and preliminary X-ray crystallographic analysis of the archaeal phosphoglycerate mutase PH0037 from *Pyrococcus horikoshii* OT3

Neratur K. Lokanath and Naoki Kunishima*

Advanced Protein Crystallography Research Group, RIKEN SPring-8 Center, Harima Institute, 1-1-1 Kouto, Sayo-cho, Sayo-gun, Hyogo 679-5148, Japan

Correspondence e-mail: kunisima@spring8.or.jp

Received 6 March 2006
Accepted 6 July 2006

Phosphoglycerate mutases catalyze the interconversion of 2-phosphoglycerate and 3-phosphoglycerate in glycolysis and gluconeogenesis pathways. The archaeal phosphoglycerate mutase PH0037 from *Pyrococcus horikoshii* OT3 has been overexpressed in *Escherichia coli* and purified. Crystals were obtained using the oil-microbatch method at 291 K. A native data set extending to a resolution of 2.2 Å has been collected and processed in space group *R*32. Assuming the presence of a dimer in the asymmetric unit, the V_M value is calculated to be 3.0 Å^3 Da^{-1}, consistent with the dynamic light-scattering experiment result, which shows a dimeric state of the protein in solution. Molecular-replacement trials using the crystal structure of *Bacilllus stearothermophilus* phosphoglycerate mutase as a search model did not provide a satisfactory solution, indicating substantially different structures of these two phophoglycerate mutases.

1. Introduction

Phosphoglycerate mutases (PGMs) catalyze the isomerization of 2- and 3-phosphoglycerates (2PGA and 3PGA) and are essential for glucose metabolism in most organisms. There are two types of PGMs: dPGM and iPGM. dPGM requires 2,3-bisphosphoglycerate (2,3-BPG) as a cofactor, while iPGM is independent of cofactor but is dependent on the presence of metal cations (Fothergill-Gilmore & Watson, 1989). From a comparison of the crystal structures of yeast and *Escherichia coli* dPGMs (Rigden *et al.*, 1998; Bond *et al.*, 2001) and iPGM from *Bacillus stearothermophilus* (Jedrzejas *et al.*, 2000), it has been concluded that these two types of PGMs are evolutionally unrelated.

In addition to their involvement in the glycolytic pathway, there is increasing evidence that dPGM/iPGM may regulate the balance between glycolysis and another ATP-producing pathway, glutaminolysis, in tumour cell lines (Kowanetz *et al.*, 2004). The iPGMs from endospore-forming Gram-positive bacteria have additional novel features in the catalytic activity of the enzymes; they absolutely and specifically require cation (Mn^{2+} or Zn^{2+}) and are extremely pH-sensitive (Singh & Setlow, 1979; Kuhn *et al.*, 1995; Chander *et al.*, 1998). These two properties appear to be both related and important in regulating the activity of these enzymes during sporulation and sperm germination (Chander *et al.*, 1998). The pH-dependency of iPGM activity is critical in the regulation of spore formation and spore germination. During the sporulation process, the developing spore or forespore will be acidified, resulting in iPGM inhibition and accumulation of 3PGA.

The iPGMs are found in all plants, selected invertebrates, certain fungi, selected algae and predominantly Gram-positive bacteria (Grana *et al.*, 1995). The metabolic importance of iPGM for some bacteria, in particular Gram-positive bacteria, and the apparent absence of iPGMs in vertebrates make this class of enzyme an ideal target for novel antibacterial drugs (Galperin *et al.*, 1998). Although several dPGM crystal structures have been reported from various organisms, *Saccharomyces cerevisiae* (Rigden *et al.*, 1998, 1999), *E. coli* (Bond *et al.*, 2001), *Mycobacterium tuberculosis* (Müller *et al.*, 2005) and human (Wang *et al.*, 2005), a crystal structure of iPGM has only been reported from *B. stearothermophilus* (Jedrzejas *et al.*, 2000;

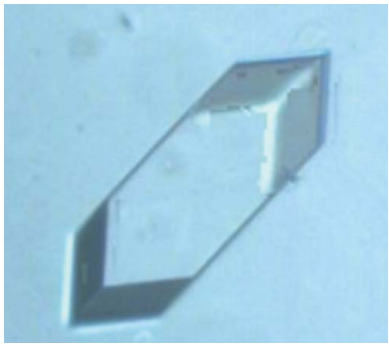

Rigden *et al.*, 2003). As part of the iPGM superfamily, an archaeal iPGM subfamily sharing 40–50% sequence identity was recently found in archaea and selected bacteria (van der Oost *et al.*, 2002). Phosphoglycerate mutase activity of the archaeal iPGMs was biochemically confirmed in those from *Methanococcus jannaschii* (Graham *et al.*, 2002) and *Sulfolobus solfataricus* (Potters *et al.*, 2003). Sequence similarity between the conventional and archaeal iPGMs are limited: the iPGM from *B. stearothermophilus* and the archaeal iPGM PH0037 from *Pyrococcus horikoshii* OT3 show only a marginal amino-acid identity of 26% (36/128) in the C-terminal domain. In order to understand the structure–function relationship of the archaeal iPGM, we decided to determine the crystal structure of this enzyme as a part of the structural genomics project in Japan (Yokoyama *et al.*, 2000). Here, we report the purification, crystallization and preliminary crystallographic analysis of the archaeal iPGM PH0037 protein from *P. horikoshii* OT3.

2. Experimental

2.1. Protein expression and purification

The PH0037 protein from *P. horikoshii* OT3 used in this study has a molecular weight of 45.4 kDa and consists of 412 amino-acid residues. Protein expression and purification were performed routinely by the Structurome Research Group in RIKEN SPring-8 Center. The plasmid encoding this protein, provided by RIKEN Genomic Sciences Center, was digested with *Nde*I and *Bgl*II and the fragment was inserted into the expression vector pET-11a (Novagen) linearized with *Nde*I and *Bam*HI. *E. coli* BL21 Codon Plus (DE3)-RIL cells were transformed with the recombinant plasmid and grown without IPTG induction at 310 K in Luria–Bertani medium containing 50 µg ml^{-1} ampicillin for 20 h. The cells were harvested by centrifugation at 4500*g* for 5 min at 277 K, suspended in 20 m*M* Tris–HCl pH 8.0 containing 0.5 *M* NaCl and 5 m*M* 2-mercaptoethanol and finally disrupted by sonication and heated at 363 K for 10 min. The cell debris and denatured protein were removed by centrifugation (18 000*g* for 30 min). The supernatant solution was used as the crude extract for purification.

The crude extract was desalted using a HiPrep 26/10 desalting column (Amersham Biosciences) and applied onto a Super Q Toyopearl 650M (Tosoh) column equilibrated with 20 m*M* Tris–HCl pH 8.0 (buffer *A*). After elution with a linear gradient of 0–0.3 *M* NaCl, the fraction containing PH0037 was desalted using a HiPrep 26/10 desalting column (Amersham Biosciences) with buffer *A*. The sample was loaded onto a Resource Q column (Amersham Biosciences) equilibrated with buffer *A*. After elution with a linear gradient of 0–0.2 *M* NaCl, the fraction containing PH0037 was desalted using a HiPrep 26/10 desalting column with 10 m*M* sodium phosphate pH 7.0. The sample was then applied onto a Bio-Scale CHT-20-I column (Bio-Rad) equilibrated with 10 m*M* sodium phosphate pH 7.0 and eluted with a linear gradient of 10–150 m*M* sodium phosphate pH 7.0. The sample was concentrated by ultrafiltration (Vivaspin) and loaded onto a HiLoad 16/60 Superdex 200 prep-grade column (Amersham Biosciences) equilibrated with buffer *A* containing 0.2 *M* NaCl. The homogeneity and identity of the purified sample were assessed by SDS–PAGE (Laemmli, 1970) and N-terminal sequence analysis. Finally, the purified PH0037 was concentrated by ultrafiltration to 30 mg ml^{-1} in buffer *A* containing 0.2 *M* NaCl.

The oligomeric state of purified PH0037 was examined by a dynamic light-scattering experiment using a DynaPro MS/X instrument (Protein Solutions), which was performed at a protein concentration of 20 mg ml^{-1} in 20 m*M* Tris–HCl pH 7.6 with 0.2 *M* NaCl. Several measurements were taken at 291 K and analyzed using the *DYNAMICS* software v.3.30 (Protein Solutions). A bimodal analysis resulted in a molecular weight of 108 kDa, which is consistent with a dimeric state of the protein in solution.

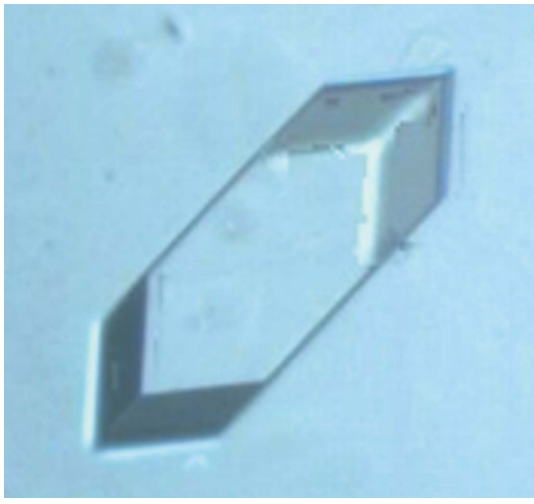

Figure 1
Crystal of the archaeal phosphoglycerate mutase PH0037. The crystal has approximate dimensions of 0.5 × 0.3 × 0.3 mm.

2.2. Crystallization

Crystallization trials were carried out using the oil-microbatch method at 291 K. Initial screening for crystallization conditions was performed using the Hampton Research Crystal Screens I and II (Jancarik & Kim, 1991). Equal volumes (1.0 µl) of protein solution and precipitant solution were mixed. The crystallization drop was overlaid with a 7:3 mixture of silicone and paraffin oils, allowing slow evaporation of water in the drop. One condition provided the largest and most well defined crystals. The precipitant solution comprised 18%(*w*/*v*) PEG 8000, 0.2 *M* calcium acetate, 0.1 *M* sodium cacodylate pH 6.5. The initial crystals were clusters of rod-shaped multiple crystals. One round of optimization resulted in large single crystals having sharp edges and dimensions of 0.3 × 0.3 × 0.2 mm (Fig. 1). These crystals typically appeared about 50 d after setup. The crystals were flash-cooled in a cryoprotectant solution consisting of the precipitant solution diluted with glycerol at 30%(*v*/*v*). Finally, the crystals were picked up in Hampton mounting loops and plunged into liquid nitrogen.

2.3. Data collection and analysis

Initial characterization of X-ray diffraction was performed using a Rigaku VII image-plate detector and Cu *Kα* X-rays (Rigaku, Japan). Autoindexing of diffraction images using *HKL*-2000 suggested a primitive rhombohedral lattice, with unit-cell parameters a = 155.62, c = 230.35 Å. Crystals were cryocooled in a nitrogen-gas steam at 100 K. X-ray diffraction intensity data were collected at SPring-8 beamline BL26B1 using a Rigaku R-AXIS V image-plate detector. A total of 180 frames were collected with 1° oscillation and 20 s exposure time per image. The wavelength of the synchrotron radiation was 1.0 Å and the crystal-to-detector distance was 270 mm. The diffraction data were integrated and scaled to 2.2 Å resolution using *DENZO* and *SCALEPACK* implemented in the *HKL*-2000 program package (Otwinowski & Minor, 1997).

Table 1
Data-processing statistics.

Values in parentheses are for the highest resolution shell.

Space group	*R*32
Unit-cell parameters (Å)	$a = b = 155.62$, $c = 230.35$
Resolution range (Å)	50.0–2.20 (2.28–2.20)
Total observations	228446
Unique reflections	54405
Redundancy	4.2 (4.3)
Completeness (%)	99.9 (100.0)
Mean $I/\sigma(I)$	11.4 (4.6)
$R_{\rm merge}$† (%)	5.0 (35.0)

† $R_{\rm merge} = \sum_{hkl}\sum_j |I_j(hkl) - \langle I(hkl)\rangle| / \sum_{hkl}\sum_j \langle I(hkl)\rangle$, where $I_j(hkl)$ and $\langle I(hkl)\rangle$ are the observed intensity of measurement j and the mean intensity of reflections with index hkl, respectively.

3. Results and discussion

The crystals obtained were found to belong to the trigonal space group *R*32, with unit-cell parameters $a = 155.62$, $c = 230.35$ Å. A complete data set was collected and the data-collection statistics are summarized in Table 1. Assuming the presence of a dimer of PH0037 in the asymmetric unit, the Matthews coefficient $V_{\rm M}$ (Matthews, 1968) was calculated to be 3.0 Å^3 Da^{-1}, corresponding to a solvent content of 58%. A dynamic light-scattering experiment shows a result consistent with a dimeric state of this protein in solution (see §2). Combining these observations, the asymmetric unit is most likely to contain a dimer of PH0037.

The sequence of the archaeal iPGM PH0037 was compared with sequences in the PDB to obtain a search model for molecular-replacement calculations. The closest homologue in the PDB is the iPGM from *B. stearothermophilus* (PDB code 1o98; Rigden *et al.*, 2003), which shares 26% amino-acid sequence identity with PH0037 in the C-terminal domain. Molecular-replacement trials were performed with *MOLREP* (Vagin & Teplyakov, 1997) using 1o98 as the search model. The top solution had $R > 0.7$ and correlation coefficient < 0.11, indicating substantially different structures for these two iPGMs. Therefore, the structure of the archaeal iPGM PH0037 will be determined by the multiwavelength anomalous dispersion method using selenomethionyl derivative crystals.

The authors would like to thank the staff of RIKEN Genomic Sciences Center for providing the plasmid and the technical staff of RIKEN SPring-8 Center for large-scale protein production and dynamic light-scattering experiments. We also thank Y. Terao for assistance during crystallization and M. Yamamoto and his staff for assistance during data collection at beamline BL26B1 of SPring-8. This work (PH0037/HTPF10012) was supported by the National Project on Protein Structural and Functional Analysis funded by the MEXT of Japan.

References

Bond, C. S., White, M. F. & Hunter, W. N. (2001). *J. Biol. Chem.* **276**, 3247–3253.
Chander, M., Setlow, B. & Setlow, P. (1998). *Can. J. Microbiol.* **44**, 759–767.
Fothergill-Gilmore, L. A. & Watson, H. C. (1989). *Adv. Enzymol. Relat. Areas Mol. Biol.* **62**, 227–313.
Galperin, M. Y., Bairoch, A. & Koonin, E. V. (1998). *Protein Sci.* **7**, 1829–1835.
Graham, D. E., Xu, H. & White, R. H. (2002). *FEBS Lett.* **527**, 190–194.
Grana, X., Perez De La Ossa, P., Broceno, P., Stocker, M., Garroage, J., Puigdomenech, P. & Climent, F. (1995). *Comput. Biochem. Physiol. B*, **112**, 287–293.
Jancarik, J. & Kim, S.-H. (1991). *J. Appl. Cryst.* **24**, 409–411.
Jedrzejas, M. J., Chander, M., Setlow, P. & Krishnaswamy, G. (2000). *EMBO J.* **19**, 1419–1431.
Kowanetz, K., Crosetto, N., Haglund, K., Schmidt, M. H., Heldin, C. H. & Dikic, I. (2004). *J. Biol. Chem.* **279**, 32786–32795.
Kuhn, N. J., Setlow, B., Setlow, P., Cammack, R. & Williams, R. (1995). *Arch. Biochem. Biophys.* **286**, 217–221.
Laemmli, U. K. (1970). *Nature (London)*, **227**, 680–685.
Matthews, B. W. (1968). *J. Mol. Biol.* **33**, 491–497.
Müller, P., Sawaya, M. R., Pashkov, I., Chan, S., Nguyen, C., Wu, Y., Perry, L. J. & Eisenberg, D. (2005). *Acta Cryst.* D**61**, 309–315.
Otwinowski, Z. & Minor, W. (1997). *Methods Enzymol.* **276**, 307–326.
Potters, M. B., Solow, B. T., Bischoff, K. M., Graham, D. E., Lower, B. H., Helm, R. & Kennely, P. J. (2003). *J. Bacteriol.* **185**, 2112–2121.
Rigden, D. J., Alexeev, D., Phillips, S. E. V. & Fothergill-Gilmore, L. A. (1998). *J. Mol. Biol.* **276**, 449–459.
Rigden, D. J., Lamani, E., Mello, L. V., Littlejohn, J. E. & Jedrzejas, M. J. (2003). *J. Mol. Biol.* **328**, 909–920.
Rigden, D. J., Walter, R. A., Phillips, S. E. V. & Fothergill-Gilmore, L. A. (1999). *J. Mol. Biol.* **286**, 1507–1517.
Singh, R. P. & Setlow, P. (1979). *J. Bacteriol.* **137**, 359–360.
Vagin, A. & Teplyakov, A. (1997). *J. Appl. Cryst.* **30**, 1022–1025.
Van der Oost, J., Huynen, M. A. & Verhees, C. H. (2002). *FEMS Microbiol. Lett.* **212**, 111–120.
Wang, Y., Wei, Z., Liu, L., Cheng, Z., Lin, Y., Ji, F. & Gong, W. (2005). *Biochem. Biophys. Res. Commun.* **331**, 1207–1215.
Yokoyama, S., Hirota, H., Kigawa, T., Yabuki, T., Shirouzu, M., Terada, T., Ito, Y., Kuroda, Y., Nishimura, Y., Kyogoku, Y., Miki, K., Masui, R. & Kuramitsu, S. (2000). *Nature Struct. Biol.* **7**, 943–945.